Biophysical Chemistry 41 (1991) 263–276
Elsevier Science Publishers B.V., Amsterdam

BIOCHE 01596

Interfacial thermodynamics of protein adsorption and ion co-adsorption. III. Electrochemistry of bovine serum albumin adsorption on silver iodide

J.G.E.M. Fraaije *, W. Norde and J. Lyklema

Department of Physical and Colloid Chemistry, Agricultural University, Dreijenplein 6, 6703 HB Wageningen (Netherlands)

(Received 7 January 1991; accepted in revised form 19 April 1991)

Abstract

An experimental analysis of charge regulation in protein adsorption is presented. The model system consists of colloidal particles of the slightly water soluble salt silver iodide as the adsorbent and the protein bovine serum albumin as the adsorbate. Protein adsorption experiments corroborate earlier findings that albumin adsorbs maximally close to the isoelectric point of the protein. The adsorption is reversible with respect to protein–protein exchange. The charge regulation is studied by novel potentiometric titrations. The Galvani potential of the adsorbent, partially covered with protein, is varied by the addition of $AgNO_3$/KI while the pH is kept constant by means of a pH-stat. It is shown that the ion co-adsorption is a linear decreasing function of the blank surface charge density. The results are consistent with thermodynamics: for the first time a few phenomenological linkage relations between the ion co-adsorptions and chemical potentials are verified experimentally. The charge regulation is interpreted in terms of a contact layer model, which explains the ion co-adsorption by compounded ion exchange equilibria in the small layer of atomic contact between adsorbed protein and surface.

Keywords: Proteins; Thermodynamics; Adsorption; Ion co-adsorption; Ion exchange; Silver iodide; Bovine serum albumin

1. Introduction

In a series of papers we addressed the interfacial thermodynamics of protein adsorption, ion co-adsorption and related issues. We recently have discussed solubilization of protein in reverse micelles [1], protein ion exchange chromatography [2,3] and the thermodynamics of ion binding to proteins in solution [4]. In this report we apply interfacial thermodynamics to a model experimental system, namely adsorption of bovine serum albumin (BSA) on the colloid silver iodide (AgI). The model experimental system is chosen such that the Galvani potential of the surface can be controlled, independently of the pH of the solution.

Albumin (human and bovine) adsorption in relation to ion co-adsorption has been studied before, using various techniques: adsorption on polystyrene (ion co-adsorption measurement by electrophoresis [5,6] and radiometry [7]) and hydrophobic copolymers (ion co-adsorption mea-

* To whom correspondence should be addressed at AKZO Corporate Research Laboratories Arnhem, Department Applied Mathematics, P.O. Box 9300, 6800 SB Arnhem, Netherlands.

surement by titration [8]). The experiments show that in many instances ion co-adsorption is not solely determined by electrostatic factors. It is well known that protein adsorption may be accompanied by (partial) unfolding and that the unfolding may lead to a shift in ion binding properties (see review [9] and references therein). Especially albumin is an interesting protein in this respect because it is a labile molecule, which has been shown to unfold on various negative surfaces in roughly the same way [9]. For pH close to the isoelectric point (i.e.p., about pH 4.7), where the protein is least labile in solution, the molecule unfolds minimally, leading to relatively high adsorbed amounts of 2–3 mg/m^2. For pH > i.e.p. or pH < i.e.p. the protein is more labile and unfolds to a larger extent, and the more so, the further the pH is away from the i.e.p., leading to relatively smaller adsorbed amounts.

The colloid AgI is one of the classical model systems from colloid chemistry (for general properties see review [10]). The colloid can be prepared as a sol or a suspension of precipitates (particle size 0.1–10μm). The precipitate lends itself to titration, by adding $AgNO_3$ and/or KI solution, without unwanted irreversible additional flocculation. Such titrations are usually analyzed in terms of the surface charge density σ_o, defined as (eq. [15] from [10]):

$$\sigma_o \equiv F(\Gamma_{AgNO_3} - \Gamma_{KI}) \qquad (1)$$

where F is the Faraday constant and Γ_i is the adsorbed amount of i in mol per square meter, σ_o is in Coulomb per square meter. Note that in the present paper, as in the previous papers [1–4] and [10], we prefer discussion of interfacial quantities in terms of adsorption of electroneutral components. However, for purpose of interpretation one may identify σ_o with the excess adsorption of Ag^+ ion minus that of I^- ion. It is not possible to discriminate between a positive adsorption of one of the components and a negative adsorption of the other.

The second experimentally observable, by the use of a AgI electrode, is the silver ion activity, expressed as $pAg \equiv -\log(a_{Ag^+})$, which can be related to the interfacial Galvani potential $\Delta\Phi$ through Nernst's Law:

$$\Delta\Phi \equiv \Phi_o + \frac{RT}{F} \ln(a_{Ag^+}) \qquad (2)$$

where Φ_o is a constant. By convention, the value of Φ_o is chosen such that $\Delta\Phi$ is zero in the zero point of charge pAg_0 of the blank in indifferent electrolyte (KNO_3).

Silver iodide has been titrated in the presences of various adsorbates, e.g. alcohols [11], polyvinylalcohols [12], tetralkylammonium nitrate salts [13], oligo- and polypeptides [14]. It is generally found that the adsorbates shift the point of zero charge to lower pAg levels, and that they decrease the differential electric capacitance. The former feature is explained by displacement of oriented surface bound water molecules by hydrophobic moieties of the adsorbates, the latter by reduction of the ratio ε_s/d_s between the dielectric constant ε_s and thickness d_s of the inner double layer part.

Here, we are interested in the titration of AgI in the presence of BSA, which may cause an additional effect. Namely, BSA contains weak acid and base side groups so that adsorbed BSA may respond to an imposed shift in Galvani potential by a shift in the acid/base equilibria, i.e. the ion co-adsorptions of acid/base and $AgNO_3$/KI may be dependent on the charge and/or potential of the surface. In our model experiment we monitor the extra uptake or release of acid/base with a pH-stat. The pH-stat introduces two additional observable quantities, namely the pH and the acid/base surface charge density σ_{ab}, defined as the excess adsorption of acid over that of base:

$$\sigma_{ab} \equiv F(\Gamma_{HNO_3} - \Gamma_{KOH}) \qquad (3)$$

As before, the adsorbed amounts are those of the electroneutral components. Negative adsorption of acid is experimentally undistinguishably from positive adsorption of base and vice versa. Bovine serum albumine does not contain hydroxyl binding sites, nor does AgI adsorb acid or base (acid or base binding is negligible for pH $\leqslant$ 7, see below). We therefore interpret σ_{ab} in terms of extra

proton charge (extra with respect to the protein in solution) of the acid/base groups of the adsorbed protein.

The AgI titration with pHstat allows us to measure in a single experiment the surface charge of the AgI colloid σ_0 and the acid/base surface charge density σ_{ab}, both as a function of the pAg (or $\Delta\Phi$) and pH. We analyze the results in two complementary ways. First, the findings are discussed with the thermodynamic method [2]. We will show that various phenomenological linkage relations between the ion co-adsorptions can actually be verified experimentally. Second, the observed behavior is explained with the contact layer model we introduced before [3]. The contact layer model explains ion co-adsorption by compounded ion exchange equilibria in the small layer of 'atomic' contact between adsorbed protein and surface. The model allows interpretation of various interesting relations, e.g. that between σ_0, σ_{ab} and the area of the contact layer.

2. Experimental

2.1 Preparation of silver iodide precipitate

We closely followed previously published procedures [10–14]. Two batches of AgI precipitate (A and B) were prepared as follows. Two liters of 0.105 *M* $AgNO_3$ were slowly added to 2 l of 0.1 *M* KI at a rate of about one drop per 10 seconds. The reaction vessel was shielded from light and continuously flushed with carbondioxide-free nitrogen in order to prevent the formation of silver oxides. After extensive washing with de-ionized water the precipitates were stored at pAg ≅ 6 in the dark under nitrogen atmosphere. Measurement of plateau adsorption of methylene blue yielded for the specific surface areas 0.25 m^2/g for precipitate A and 0.30 m^2/g or precipitate B. The latter precipitate was used for the titrations and protein plateau adsorption measurements. The point of zero charge of precipitate B was 5.80, very close to the literature value 5.67. From capacitance measurement in the point of zero charge in dilute KNO_3 (1.1 m*M*) we calculated a specific surface area of 0.88 m^2/g (for method see [10]). The discrepancy between the two estimates of the specific surface has been found before [10–14]; no satisfactory explanation has been given so far. In this report we prefer using the area from the dye adsorption measurement. In the Results section (Section 3) we will discuss this choice in some more detail.

2.2 Preparation of BSA

Bovine serum albumin was purchased from Sigma (type VI, γ-globuline and fatty acid free). The number of sulfhydryl groups per protein molecule was initially between 0.3 and 0.4. We increased the sulfhydryl content by a purification method [15]; after purification the number was between 0.85 and 0.88. The sulfhydryl group was subsequently blocked by carboxyamidation, either with normal or radioactive iodoacetamide (C^{14}) [15]. The protein, freed from salt and freeze-dried, was stored at −20 °C.

2.3 Adsorption isotherms

Typically, 0–5 ml of protein solution (containing 0–3 mg of BSA in 0.1 *M* KNO_3) were added to 5 ml of well dispersed AgI precipitate (containing 1.7 g AgI in 0.1 *M* KNO_3) in 10 ml Sybron/Nalge polycarbonate centrifuge tubes. After the total volumes of the tubes had been adjusted to 10 ml with 0.1 *M* KNO_3 solution, the tubes were stoppered with polyethylene caps and vigorously shaken for 10 seconds on a whirl mixer. The tubes were then rotated end over end for 16 hours to reach steady state (more than 90% of the final protein adsorption was already reached in less than a quarter of an hour). Next, the tubes were centrifuged for 20 minutes at 20,000 rpm in a Beckman JA-21 centrifuge equipped with a JA-21 rotor. The protein concentration in the supernatant was determined by measuring the absorbance at 280 nm.

2.4 Protein–protein exchange

First, 5 ml of unlabelled BSA (2 mg/ml) was added to 25 ml of dispersed AgI precipitate (solid contents 0.37 gram/ml) in a 50 ml Schott/Duran flask. The mixture was then vigorously stirred for 16 hours using a magnetic stirrer. After the pro-

tein adsorption had been determined, a small amount of radioactive BSA was added, less than 5% of the total amount of protein already present, and the stirring was continued. At selected time intervals 0.5 ml aliquots were taken from the dispersion and centrifuged in a top desk centrifuge in 1 ml polyethylene vials. The concentration of radioactive BSA was determined with a scintillation counter. The adsorptions of radioactive and unlabelled BSA were calculated from the respective depletions.

2.5 Titration, instrumentation

The titrations were carried out in a thermostatted (20 °C) Schott titration vessel (volume 150 ml). The vessel was equipped with four AgI electrodes fitted in one holder, a Schott pH glass electrode and a so-called Van Laar salt bridge (see reference 120 in [10] for original details) with resistance 700 kΩ. The reference chamber contained saturated KCl and a Schott Ag/AgCl reference electrode. The electrode potentials were measured with a multichannel voltage meter (HP 3497A Data Acquisition/Control Unit) after they had been converted to low impedance signals with a home-built impedance transformer. The titrants ($AgNO_3$ and KI both 0.01 *M* in 0.1 *M* KNO_3, HNO_3 and KOH both 0.025 *M* in 0.1 *M* KNO_3) were added with a Metrohm 655 Dosimat. Homogenization of the concentrated dispersion (about 30% by weight) was achieved by stirring vigorously at the bottom and top of the vessel. The experiments were automated by means of a HP 85 microcomputer. Every five minutes, the computer program collected the data from the electrodes, averaged the signals from the four independent AgI electrodes, decided whether equilibrium had set in (tolerated drifts 0.001 pH/min and 0.001 pAg/min, tolerated spread between the AgI electrodes 0.02 pAg), ordered the burets to add small aliquots of titrant (0.01–0.1 ml) if necessary, and stored the data.

2.6 Titration, calibration

The AgI electrodes were calibrated by short titrations (from 10^{-5} to $5 \cdot 10^{-3}$ *M*) with $AgNO_3$ and KI solution in 0.1 *M* KNO_3 solution. The effect of pH on the E_0 values was negligible (< 1 mV) within the pH range we studied ($4 \leqslant pH \leqslant 7$), conversely, the pH drift during the AgI electrode calibration was also negligible (< 0.01 pH unit in unbuffered pH 5.5 solution). The AgI solubility product p*S* was 16.03–16.06, slightly lower than the literature value 16.07 [10]. The pH electrode was calibrated with commercial buffers (Titrisol) of pH 4 and pH 7. The pH and AgI electrode calibrations were repeated directly before and after every AgI titration.

2.7 Titration, procedure

First, wet AgI precipitate was added to the titration vessel to a final amount of 28–30 gram, dispersed in 100 ml 0.1 *M* KNO_3 and adjusted to pAg 5.5 and selected pH. Then a blank titration was carried out, up to pAg 10.5, in nine steps by successive addition of KI titrant. Next, the titration was reversed in one step by the addition of $AgNO_3$ titrant. The initial pAg was always recovered within 0.02 pAg unit. Then 2 mg BSA was added as 1 ml freshly prepared protein solution in 0.1 *M* KNO_3 and also at the selected pH level ($\pm$0.001 pH unit). Any pH changes in the titration vessel were first corrected by the pHstat and then the KI titration was repeated. During the titration, the pH-stat continuously monitored the pH, and corrected drifts of pH by addition of the acid and/or the base titrant. In the experiments described, the pH-stat tolerance was set to (in units of pH): 0.001 (pH 4), 0.003 (pH 5) and 0.01 (pH 6).

The total procedure for one titration curve took 6–8 hours, the scheme was repeated several times with increasing loads of BSA.

3. Results

3.1 Adsorption isotherms

Some typical adsorption isotherms are presented in Fig. 1 as a function of initial pH and pAg. The specific surface area we used for the calculation of the adsorption values in mg/m^2

was from the dye plateau adsorption measurement (0.25 m^2/g for precipitate A), as explained in the experimental section. The protein plateau adsorption values (see also Fig. 2) range from 1–2.5 mg/m^2, in fair agreement with commonly accepted plateau adsorption values of albumin [9]. If we would have used the surface area (0.88 m^2/g) from the capacitance measurement, then the plateau values would have been in the range 0.3–0.8 mg/m^2, which is obviously too low.

The adsorption isotherms of Fig. 1 reveal that up to about 75% of the plateau adsorption the bulk concentration is below 0.001 mg/ml (detection limit). The isotherms are for four different combinations of initial pH and pAg, including adsorption of (almost) uncharged protein on (almost) uncharged AgI (pH 5, pAg 6.1) and at the other extreme adsorption of negative protein on (very) negative AgI (pH 7, pAg 10.1). The adsorption clearly remains of the high affinity character, even for the case where negative BSA adsorbs on negative AgI.

We found that after protein adsorption the equilibrium pH and pAg levels where slightly shifted (less than 1 pH or pAg unit) from the initial values, indicating that the protein adsorption was accompanied by ion co-adsorption. In general, these shifts were similar to those measured more directly in the titration experiments described below.

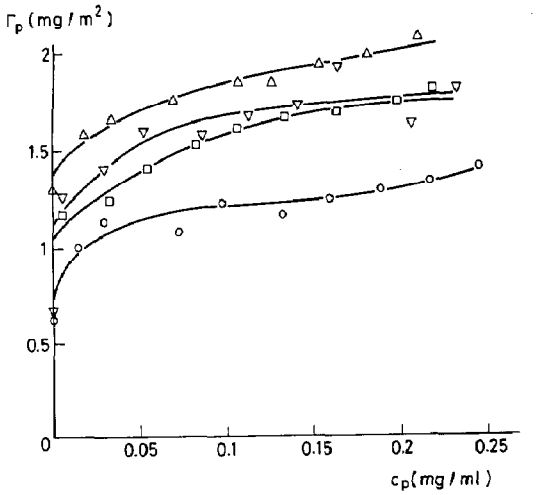

Fig. 1. Adsorption Γ_p of BSA on AgI vs. equilibrium concentration c_p in 0.1 M KNO_3. Initial pAg, pH values: (▽) pAg 6.1, pH 7; (○) pAg 10.1, pH 7; (△) pAg 6.1, pH 5; and (□) pAg 10.1, pH 5.

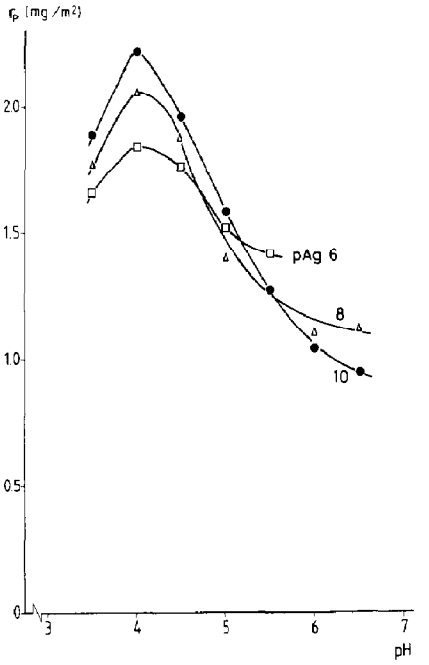

Fig. 2. Plateau adsorption of BSA on AgI vs. equilibrium pH and pAg (interpolated, see text) in 0.1 M KNO_3.

3.2 Plateau adsorption

In a separate experiment we varied the initial pH and pAg (in a matrix of 11 points variation in pH vs. 4 points variation in pAg, i.e. in total 44 points), while the total amount of protein was held constant (2.5 mg). The equilibrium protein concentration in bulk varied with adsorbed amount from 0.11 mg/ml to 0.2 mg/ml, this is in the plateau regime (Fig. 1). These adsorption values were (graphically) interpolated with respect to the equilibrium pH and pAg values, to values for constant pH and pAg. The results are shown in Fig. 2. The curves show that the adsorption is a maximum at pH 4, close to, but slighly lower than the i.e.p. We noted already in the Introduction that Albumin adsorbs on a variety of negative surfaces with maxima close to the i.e.p. of the protein (pH 4.7) [9], our results confirm this. There is a small effect of the surface charge:

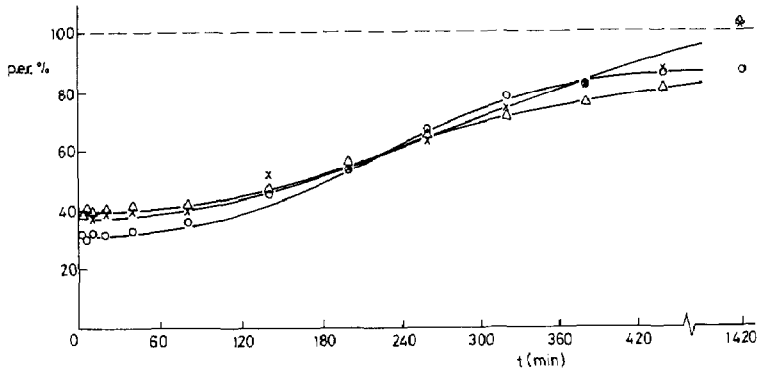

Fig. 3. Protein exchange ratio p.e.r. vs. exchange time. 0.01 M KNO_3, pAg 10: (○) pH 6, $c_p = 0.08$ mg/ml; (×) pH 5, $c_p = 0.07$ mg/ml; (△) pH 4, $c_p = 0.03$ mg/ml.

we find that the adsorption is slightly higher when the charges of protein and surface are opposite.

3.2 Protein–protein exchange experiments

As a measure of the protein exchange we used the protein exchange ratio (p.e.r.) $\equiv (\Gamma/c)_{\text{radioactive BSA}} \times (c/\Gamma)_{\text{unlabelled BSA}}$. The dependence of p.e.r. on the medium conditions and time is depicted in Fig. 3. The results clearly indicate that the adsorption is reversible, with a rapid exchange to p.e.r. ≅ 30–40% in the first few minutes, and a slower exchange to p.e.r. ≅ 100% in the following hours. Moreover, there is little influence of the pH. This demonstration of reversibility is important: it is a prerequisite to verify the thermodynamic linkage relations in the Discussion.

3.3 Titrations

The titration curves are shown in Fig. 4. Adsorption of the protein is reflected in the shifts in σ_o and σ_{ab} with respect to the blank values. Note

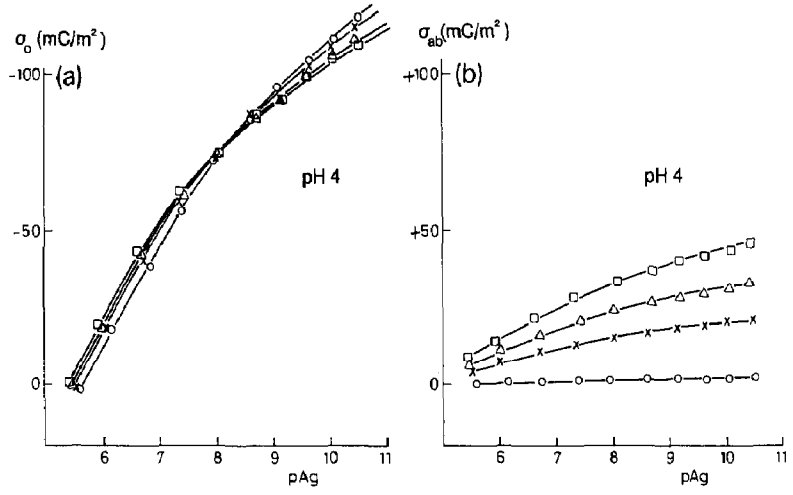

Fig. 4. Titration of AgI–BSA complex in 0.1 M KNO_3 at fixed pH, σ_o is surface charge density of AgI (eq. [1]), σ_{ab} is acid/base surface charge density (eq. [3]). pH 4 and pH 5: (○) blank; (×) $\Gamma_p = 0.47$ mg/m^2; (△) $\Gamma_p = 0.93$ mg/m^2; and (□) $\Gamma_p = 1.4$ mg/m^2. ph 6: (○) blank; (×) $\Gamma_p = 0.33$ mg/m^2; (△) $\Gamma_p = 0.67$ mg/m^2; and (□) $\Gamma_p = 0.93$ mg/m^2.

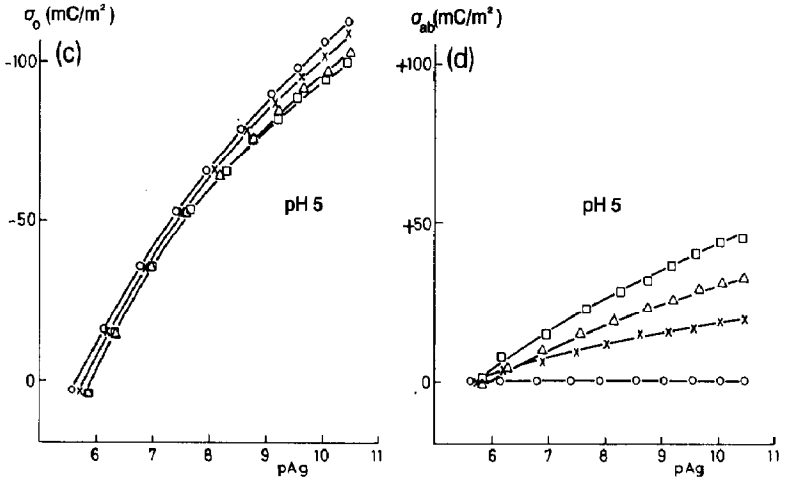

Fig. 4. (continued).

that in these experiments the protein adsorption levels are below the plateau adsorption values and that consequently the protein concentration in solution is negligibly low. We may therefore identify the charge regulation with the response of adsorbed protein only and neglect contributions from titration of the protein in solution.

The blank curves of σ_0 for the different pH levels are identical, illustrating the absence of base/acid adsorption on the bare AgI surface. This is confirmed by the (undetectably) low acid/base adsorption σ_{ab} in the blank titration. The shapes of the blank σ_0 curves are in good agreement with published titration curves of AgI precipitates in 0.1 M KNO_3, although the absolute values from our measurements are about a factor 3 higher [10]. The explanation lies in the discrepancy between the specific surface area from capacitance measurement (often used in the older work [10], 0.88 m^2/g for the precipitate B), whereas here we prefer to use the specific surface area from the dye adsorption measurement (0.30

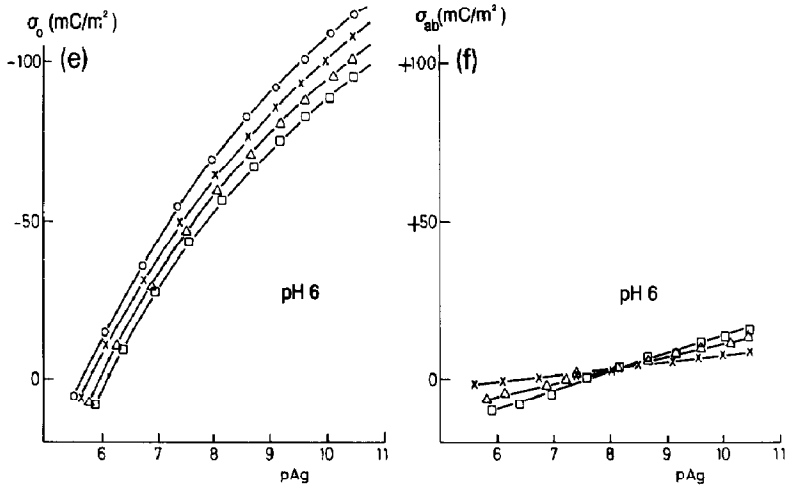

Fig. 4. (continued).

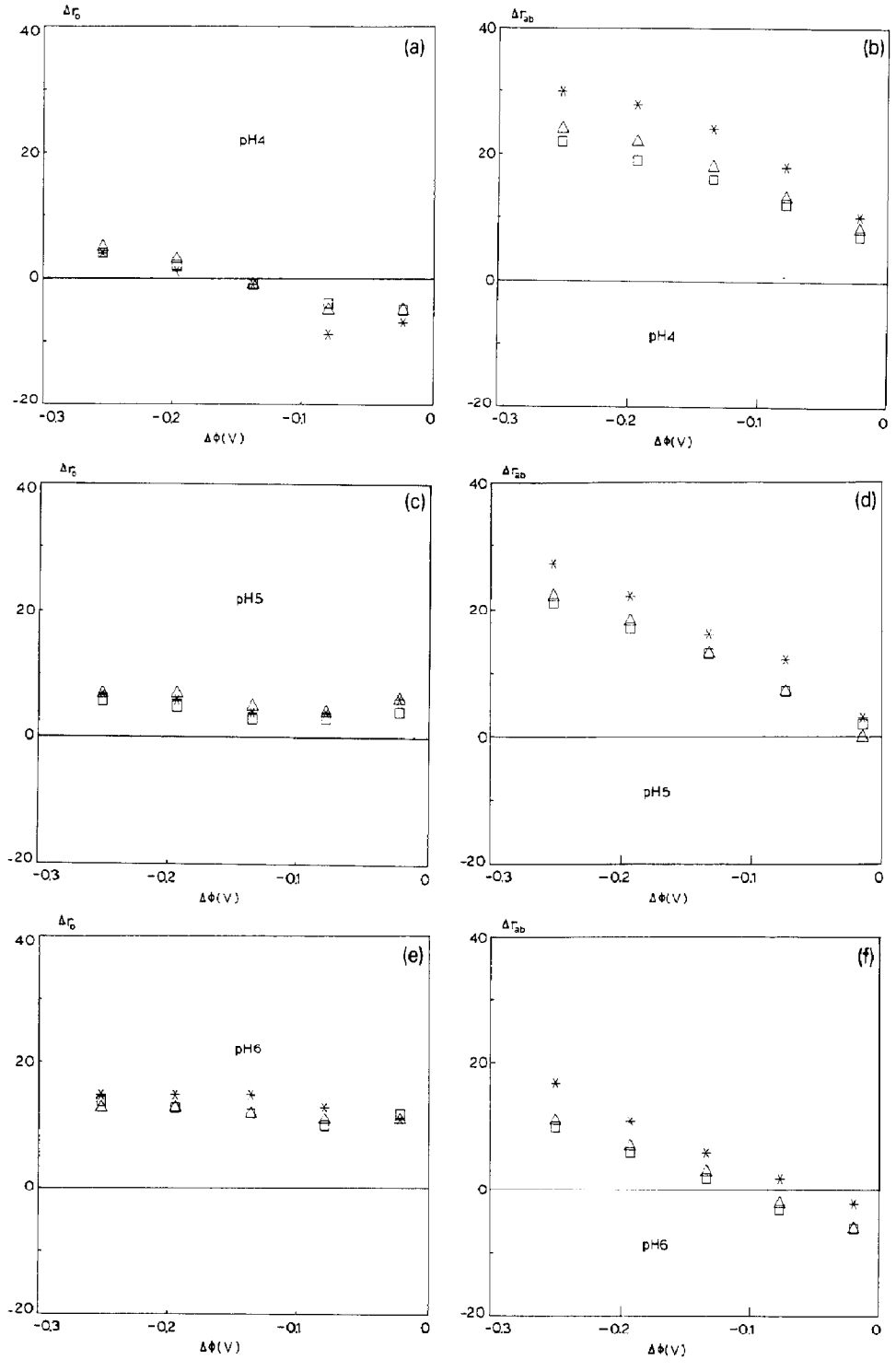

Fig. 5. Ion co-adsorption numbers Δr_i vs. interfacial Galvani potential $\Delta\Phi$. pH 4 and pH 5: (○) blank; (∗) $\Gamma_p = 0.47$ mg/m^2; (△) $\Gamma_p = 0.93$ mg/m^2); and (□) $\Gamma_p = 1.4$ mg/m^2. pH 6: (○) blank; (∗) $\Gamma_p = 0.33$ mg/m^2; (△) $\Gamma_p = 0.67$ mg/m^2; and (□) $\Gamma_p = 0.93$ mg/m^2.

m^2/g for the precipitate B). Note that we do so in order to make the BSA plateau adsorption levels conform to the literature values.

We find that in general the more negatively charged protein (pH 6) makes σ_o more positive, and that the more positively charged protein (pH 4) makes σ_o more negative (except for pAg > 8.5). Also, in all cases a more negatively charged surface makes the protein more positive. These effects are clearly a result of electrostatic induction. Note however that for pH 4 (Fig. 4a) there is a common intersection point (c.i.p.) in the σ_o curves (around pAg 8.5), such that for pAg > c.i.p. the surface, partially covered with positively charged protein, is *less* negatively charged than the blank.

A second feature is that the differential electric capacitance C ($\equiv \partial\sigma_o/\partial\Delta\Phi = -17.19\ \partial\sigma_o/\partial$pAg in F/m^2) is not much affected by the protein adsorption. Comparison with effects of other types of adsorbates [10–14] shows that in this respect BSA behaves exceptionally (see Introduction). In general, the effect of an adsorbate is to reduce C significantly, which is explained by a possible increase in the thickness of the Stern layer and/or lowering of relative dielectric constant of the Stern layer. The implicit assumption is then that the Stern layer itself cannot adjust in charge, i.e. is not titratable. Here, the adsorbed protein readily adjusts its charge through titration of the acid/base groups in the contact zone between protein and surface, which is the region dominating C.

3.4 Ion co-adsorption numbers

A slightly different presentation of the titration results, especially suited for the thermodynamic and model interpretation, is in terms of the ion co-adsorption numbers of the acid/base, Δr_{ab}, and $AgNO_3$/KI, Δr_o. These are the numbers of ions extra adsorbed or desorbed per adsorbed protein molecule. They are defined through:

$$\Delta r_o \equiv \frac{1}{F\Gamma_p}\left(\sigma_o - \sigma_o^b\right) \tag{4a}$$

$$\Delta r_{ab} \equiv \frac{1}{F\Gamma_p}\sigma_{ab} \tag{4b}$$

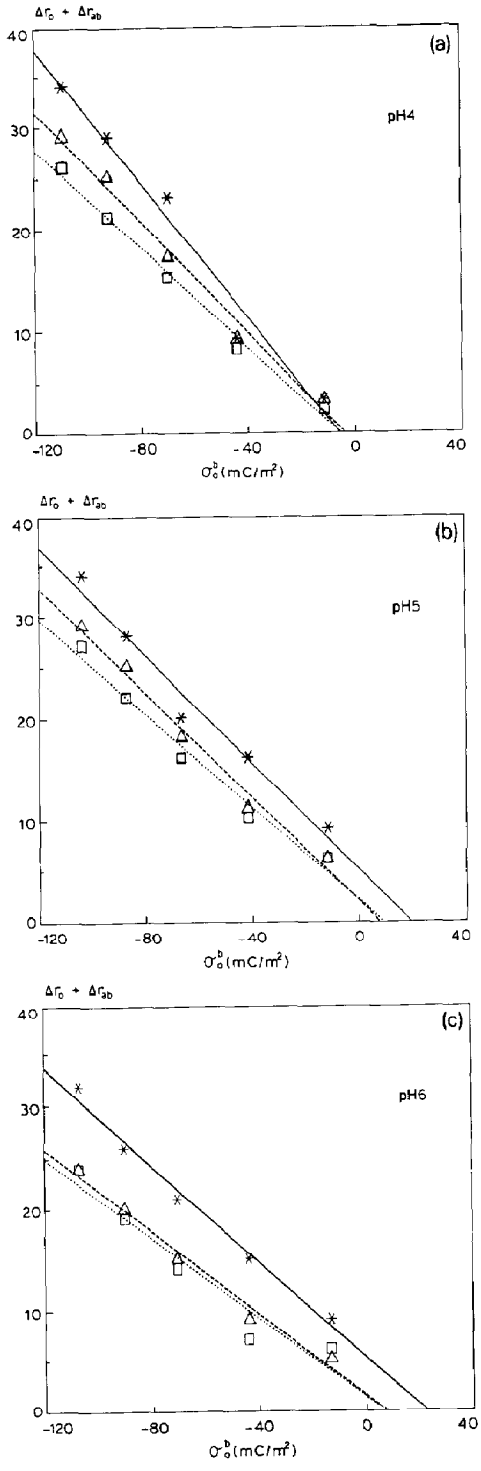

Fig. 6. Total ion co-adsorption $\Delta r_o + \Delta r_{ab}$ vs. surface charge density of the blank σ_o^b. Symbols as in Fig. 5.

where σ_o^b is the surface charge density of the blank. The co-adsorption numbers were calculated from the original titration curves Figs. 4 through graphical interpolation. The results are shown in Figs. 5 (note that we have also converted pAg to the Galvani potential by the use of eq. [2] and $pAg_0 = 5.67$ for the blank).

We recall from the proton titration experiments by Tanford [12] that the isoionic point of BSA in solution is about pH 5.5–5.6 and the isoelectric point is about 4.7. The proton binding number is about 29–34 for pH 4, 6–7 for pH 5 and −3 for pH 6 (lower numbers measured in 0.08 *M* KCl, higher numbers in 0.15 *M* KCl). The maximum positive proton binding number is about 96, i.e. this number of protons may be bound in excess to the isoionic state [4]. This implies that the maximum number the protein can co-adsorb is about 62–67 at pH 4, 89–90 at pH 5 and 99 at pH 6. The co-adsorption curves show that in the present case the co-adsorption levels are far below the maximally attainable levels, indicating that in principle the protein has ample capacity to adjust in charge by the extra uptake or release of protons. However, it is possible that the saturation observed near $\Delta r_{ab} \cong 30$ for pH 4–5 (Figs. 5b,d) indicates that the effective maximally attainable co-adsorption numbers are smaller than the theoretical values we calculated. This may be explained by the contact layer model in which only a fraction of the total number of acid/base groups of the protein is affected by the surface and, hence, may contribute to the co-adsorption.

An alternative plot is that of the total co-adsorption $\Delta r_o + \Delta r_{ab}$ vs. σ_o^b (Fig. 6), calculated from Fig. 4 through graphical interpolation, using eqs. (4). We find that, within experimental accuracy, the total ion co-adsorption is a linearly decreasing function of the surface charge density of the blank (the data from linear regression analysis are collected in Table 1). This is a surprising and unexpectedly simple result for such a complicated system. As far as we know, this is the first time the effect has been noted. We will come back to it in more detail in the Discussion below.

4. Discussion

4.1 Thermodynamic interpretation

Generally speaking, thermodynamics predicts that co-adsorption numbers and chemical potentials are related through various Maxwell (or linkage) equations. These equations are easily derived from a set of coupled Gibbs–Duhem relations, as we have shown in [2]. In the Appendix the theory is applied to find the linkage relations between the co-adsorption numbers Δr_o and Δr_{ab}

Table 1

Regression analysis of $\Delta r_o + \Delta r_{ab}$ vs. σ_o^b (Fig. 6)

Γ_p (mg/m^2)	R^2	Intercept	Slope	
			(m^2/mC)	(nm^2/molecule)
pH 4				
0.47	0.97	−2.4	−0.33	53
0.93	0.99	−1.6	−0.27	44
1.4	0.99	−1.9	−0.25	39
pH 5				
0.47	0.96	4.9	−0.26	42
0.93	0.99	1.7	−0.26	41
1.4	0.98	1.8	−0.23	37
pH 6				
0.33	0.99	5.1	−0.24	38
0.67	0.98	1.3	−0.20	33
1.0	0.93	1.3	−0.20	32

Table 2

Experimental verification of linkage relation eq. (5a) [a]. Conditions: $\Gamma_p = 1.0$ mg/m^2, pH 5

pAg	$\left(\frac{\partial \Delta r_{ab}}{\partial pAg}\right)_{\Gamma_p,pH}$	$\left(\frac{\partial \Delta r_o}{\partial pH}\right)_{\Gamma_p,pAg}$
6	9.0	9.4
7	8.2	8.9
8	7.0	6.0
9	6.5	5.4
10	5.3	4.2
average	7.2	6.8

[a] Experimental accuracy of the listed differential coefficients is 0.5–1 unit; the accuracy of the averages is 0.3–0.4 unit.

and the ion activities a_{H^+} and a_{Ag^+}. Two linkage relations are of special interest because they can experimentally be verified. The relations are, assuming the salt activity is constant:

$$\left(\frac{\partial \Delta r_{ab}}{\partial pAg}\right)_{\Gamma_p,pH} = \left(\frac{\partial \Delta r_o}{\partial pH}\right)_{\Gamma_p,pAg} \quad (5a)$$

$$\left(\frac{\partial \Delta r_{ab}}{\partial \Delta r_o}\right)_{\Gamma_p,pH} = -\left(\frac{\partial pAg}{\partial pH}\right)_{\Gamma_p,\Delta r_o} \quad (5b)$$

Equation (5a) was tested by combination of the co-adsorption curves in Figs. 5 for $\Gamma_p = 1.0$ mg (pH 4 and 5) and $\Gamma_p = 0.93$ (pH 6) by a finite difference scheme, neglecting the small difference in the protein adsorbed amounts (the effect of Γ_p on the co-adsorption numbers is small anyway). The left-hand side (l.h.s.) was calculated for various values of pAg ($\Delta\Phi$) from the isopH Δr_{ab} curve for pH 5. The right-hand side (r.h.s.) was approximated by central difference between the pH 4 and pH 6 curves. The results, shown in Table 2, indicate that the linkage relation eq. (5a) is indeed obeyed; the average values of the l.h.s and r.h.s do not differ more than 6%, which is about the experimental accuracy.

The l.h.s of eq. (5b) was calculated directly from the ratio of the slopes of the Δr_o and Δr_{ab} curves from Figs. 5 (pH constant). The r.h.s was calculated from combination of detailed data from the pH-stat. Specifically, the δpH shifts induced by addition of the KI titrant were always small, usually less than 0.1 pH unit. These shifts were corrected by the pH-stat, which resulted in turn in small shifts δpAg, usually less than 0.05 pAg unit. The shifts δpAg induced by the pH-stat were always concomitant with very small shifts in Δr_o (less then 0.1 co-adsorption unit), such that $\Delta r_o \cong$ constant. We therefore approximated the differentials ∂pH and ∂pAg in the r.h.s of eq. (5b) by ∂pH and ∂pAg respectively. Closer inspection showed that these detailed data were too inaccurate for test of the linkage relation in each individual point in the titration curves. We performed a statistical analysis of the ratio of the l.h.s by the r.h.s of eq. (5b) and found that the ratio was approximately normal distributed, indicative of random errors, with an average value of 0.96 and standard deviation of about 1.06 (calculated from 241 pH adjustment cycles). We take this as evidence that eq. (5b) is also obeyed.

4.2 Model interpretation

According to the contact layer model [3], the charge regulation is confined to the small layer of 'atomic' contact between protein and surface. An additional premise is that the contact layer as a whole is electroneutral. The latter requirement is fulfilled when the protein body electrostatically shields the contact layer from the solution completely. This can be checked by measuring the ζ-potential in an electrophoresis experiment: if the contact layer is shielded then the surface, fully covered with protein, should titrate as the protein in solution. Some years ago, Norde has shown this to be the case for albumin adsorption on polystyrene [9]. We assume that the same type of shielding mechanism applies also to Albumin adsorption on AgI.

In the present case an additional complication has to be considered, namely that the solution side of the adsorbed protein binds Ag^+ and/or I^-. We measured the Ag^+/I^- binding capacity of BSA in solution by a few additional titration experiments in the range pH 6–8 and pAg 4–6. Figure 7 shows that the Ag^+ binding rapidly increases with increasing pH and decreasing pAg, indicative of pH-controlled complexation, possibly with amine containing residues [19]. However, under the conditions prevailing in the AgI experi-

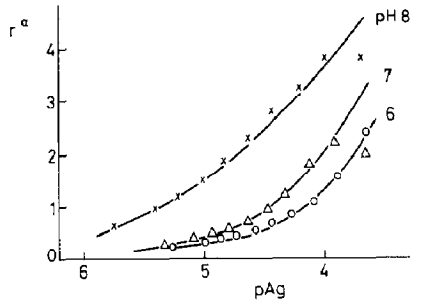

Fig. 7. Number r^{α} of Ag^+ ions bound by BSA in solution, 0.1 *M* KNO_3, vs. pAg. pH indicated. BSA concentration is 1 mg/ml.

ments the Ag^+ binding may be neglected. The I^- binding was below the detection limit.

The implementation of the contact layer model is as follows. The number of surface charges in the contact layer r_o^c is the number already present in the blank plus the number of co-adsorbed surface charges:

$$r_o^c = \Delta r_o + a_p \frac{\sigma_o^b}{F} \tag{6}$$

where a_p is the area of the contact layer. Note that the binding and co-adsorption numbers are dimensionless, a_p is in m^2/mol.

We assume that a fraction f of the acid/base groups of the protein is in the contact layer. This fraction is related to the area a_p by some geometrical factor, but here we do not need to impose such a relation: f and a_p can in principle be estimated separately. The number of excess protons in the contact layer r_{ab}^c is the fraction f of the proton binding number in solution plus the number of co-adsorbed protons:

$$r_{ab}^c = \Delta r_{ab} + f r_{ab}^{\alpha} \tag{7}$$

where r_{ab}^{α} is the acid/base (proton) binding number in solution.

Co-adsorbed electrolyte introduces an additional number of charges r_s^c in the contact layer. The number r_s^c is defined as the excess number of incorporated K^+ over that of NO_3^-:

$$\begin{aligned} r_s^c &\equiv r_{K^+}^c - r_{NO_3^-}^c \\ r_{K^+}^c &\equiv r_{KNO_3}^c + r_{KOH}^c + r_{KI}^c \\ r_{NO_3^-}^c &\equiv r_{KNO_3}^c + r_{HNO_3}^c + r_{AgNO_3}^c \end{aligned} \tag{8}$$

Combination of eqs. (1,3,6–8) gives the basic expression for the charge balance in the contact layer:

$$\Delta r_o + \Delta r_{ab} = -f r_{ab}^{\alpha} - a_p \sigma_o^b / F - r_s^c \tag{9}$$

Experimentally it was found (Fig. 6) that $\Delta r_o + \Delta r_{ab}$ is a linearly decreasing function of the blank surface charge density; this would indicate that f, a_p and r_s^c do not significantly depend on the Galvani potential so that they can be calculated directly from the data from Table 1. A few features are noteworthy:

(i) Slope. The values for a_p are realistic. The (native) shape of Albumin is that of a prolate spheroid, with dimensions $1.7 \times 2.7 \times 11.6$ nm (unhydrated) [17], or according to another estimate $4 \times 4 \times 14$ nm (hydrated) [18]. The projection area of such an ellipsoid, adsorbed sideways on a surface, would be between 26 nm^2 (unhydrated) and 44 nm^2 (hydrated). This is in the range of the a_p values listed in Table 1. The higher values of a_p, especially compared with the unhydrated native dimensions, indicate to some unfolding. An additional feature is that a_p is (slightly) dependent on Γ_p, such that the higher the adsorbed amount, the smaller a_p is. A tentative explanation would be that the protein is more unfolded when the surface concentration is low, and that with increasing adsorption the unfolding decreases in order to accommodate more molecules on the surface. There also is the trend that a_p is highest for pH 4. Tanford has shown that BSA undergoes reversible expansion below pH 4.3 [16]; such expansion could be facilitated by surface–protein interactions.

(ii) Intercept. The accuracy of the intercepts (Table 1) is limited (a few co-adsorption units) but it is clear that the intercept is slightly negative for pH 4 and slightly positive for pH 5 and 6. The values for the proton binding numbers in solution are (see above) 29–34 (pH 4), 6–7 (pH 5) and −3 (pH 6). We do not have independent information on f and r_s^c but a rough estimate for r_s^c can be obtained as follows. Suppose, for sake of argument, that the shape of the adsorbed protein is that of a flattened ellipsoid, such that the entire part of the molecule which is oriented to the surface is in the contact zone. In this

picture f would be about 0.5. Combination of the average values for the intercepts with the proton binding numbers gives: $r_s^c \cong -13$ to -15 (pH 4), -6 (pH 5), -4 (pH 6). The fact that these data are negative means that there is a preference for accumulation of anions NO_3^- in the contact layer. It is well known that KNO_3 is an almost perfect indifferent electrolyte for AgI; the specific interaction of K^+ and/or NO_3^- with the AgI surface is very small [10]. On the other hand, BSA does bind anions specifically [4,16], especially in acid media. It is therefore possible that the protein retains some of its bound NO_3^- when it adsorbs. In this picture, the NO_3^- ions would partly be incorporated in the contact layer, in proportion to the fraction of acid/base groups in the contact layer. Previously [4], we calculated the anion binding capacity of albumin through a thermodynamic interpretation of the Tanford titration data. For Cl^- binding in 0.07 M KCl we found: anion binding $\cong 25$ (pH 4), 7.5 (pH 5) and -1 (pH 6). When a fraction $f \cong 0.5$ of these anions incorporates in the contact layer then $r_s^c \cong -12.5$ (pH 4), -3.3 (pH 5) and $+0.5$ (pH 6); this is in fair agreement with the values calculated above.

5. Conclusions

We have demonstrated that charge regulation in protein adsorption can be quantified experimentally by pH-stat controlled AgI titrations. The experiments show that the proteins exchange reversibly between the adsorbed and dissolved state and that the charge regulation is consistent with thermodynamics. The experimental linear relation between the total ion co-adsorption and the surface charge density of the blank can be interpreted with a simple model, in which the charge regulation is confined to the layer of contact between protein and surface.

We did not address model interpretation of the shifts of Galvani potential and interfacial capacitance in relation to the ion co-adsorption. This requires extension of the model to specify exactly where the ions are incorporated in the contact layer. In a following publication we will come back to this problem.

Acknowledgements

The research was made possible by financial support from the Netherlands Organization for Scientific Research (NWO). M. Bakkenes and A. Korteweg are acknowledged for technical assistance, G. Buurman and A. Hoekstra for preparing some of the figures.

Appendix

The linkage relations can be derived from a set of coupled Gibbs–Duhem relations for a system in which the surface–protein solution is in membrane equilibrium with its dialysate [2]. Here, we identify the blank as the thermodynamic reference. The differential of the surface pressure π^s is (eq. (A7) from [2], for the case $c_w \gg c_i$):

$$\begin{aligned} d\pi^s = {} & \Gamma_p \Delta r_{HNO_3}\, d\mu_{HNO_3} + \Gamma_p \Delta r_{KOH}\, d\mu_{KOH} \\ & + \Gamma_p \Delta r_{KNO_3}\, d\mu_{KNO_3} + \Gamma_p \Delta r_{AgNO_3}\, d\mu_{AgNO_3} \\ & + \Gamma_p \Delta r_{KI}\, d\mu_{KI} + \frac{\Gamma_p}{c_p}\, d\pi \end{aligned} \tag{A1}$$

where $\pi^s \equiv \gamma - \gamma^o$, γ is the surface tension of the AgI surface (partly) covered with protein, γ^o is the surface tension of the blank surface and π is the osmotic pressure between the surface–protein solution and its dialysate. In the present case the salt activity is constant ($c_s = 0.1$ M), so that $d\mu_{KNO_3} = 0$, $d\mu_{HNO_3} = -d\mu_{KOH} = RT\, d\ln(a_{H^+})$ and $d\mu_{AgNO_3} = -d\mu_{KI} = RT\, d\ln(a_{Ag^+})$. Using the definitions (1, 3, 4) we find:

$$\begin{aligned} d\pi^s = {} & RT\Gamma_p \Delta r_{ab}\, d\ln(a_{H^+}) \\ & + RT\Gamma_p \Delta r_o\, d\ln(a_{Ag^+}) \\ & + \frac{\Gamma_p}{c_p}\, d\pi \end{aligned} \tag{A2}$$

The linkage relations eqs. (5a–b) are obtained by a few additional Legendre transformations and subsequent cross-differentiations. Equation (5a) is found from the differential of $\pi^s - (\Gamma_p/c_p)\pi$ and eq. (5b) from the differential of $\pi^s - (\Gamma_p/c_p)\pi - RT\Gamma_p \Delta r_o \ln(a_{Ag^+})$.

References

1 J.G.E.M. Fraaije, E.-J. Rijnierse, R. Hilhorst and J. Lyklema, Colloid Polym. Sci. 268 (1990) 855.
2 J.G.E.M. Fraaije, R.M. Murris, W. Norde and J. Lyklema, Biophys. Chem. 40 (1991) 303.
3 J.G.E.M. Fraaije, W. Norde and J. Lyklema, Biophys. Chem. 40 (1991) 317.
4 J.G.E.M. Fraaije and J. Lyklema, Biophys. Chem. 39 (1991) 31.
5 W. Norde and J. Lyklema, J. Colloid Interface Sci. 66 (1978) 277.
6 A.V. Elgersma, R.L.J. Zsom, W. Norde and J. Lyklema, J. Colloid Interface Sci., 138 (1990) 145.
7 P. van Dulm, W. Norde and J. Lyklema, J. Colloid Interface Sci. 82 (1981) 77.
8 H. Shirahama, T. Shikuma and T. Suzawa, Colloid Polym. Sci. 267 (1989) 587.
9 W. Norde, Adv. Colloid Interface Sci. 25 (1986) 267.
10 B.H. Bijsterbosch and J. Lyklema, Adv. Colloid Interface Sci. 9 (1978) 147.
11 B.H. Bijsterbosch and J. Lyklema, J. Colloid Interface Sci. 20 (1965) 665.
12 L.K. Koopal and J. Lyklema, Faraday Discuss. Chem. Soc. 59 (1975) 230.
13 A. de Keizer and J. Lyklema, J. Colloid Interface Sci. 75 (1980) 171.
14 H.A. van der Schee and J. Lyklema, in: The effect of polymers on dispersion properties, ed. Th.F. Tadros (Academic Press, New York, NY, 1982) p. 81.
15 J. Janatova, J.K. Fuller and M.J. Hunter, J. Biol. Chem. 243 (1968) 3612.
16 C. Tanford, S.A. Swanson and W.S. Shore, J. Am. Chem. Soc. 77 (1955) 6421.
17 C.L. Ridiford and B.R. Jennings, Biochim. Biophys. Acta 126 (1966) 71.
18 P.G. Squire, P. Moser and C.T. O'Konski, Biochem. J., 7 (1968) 426.
19 J. Steinhardt and S. Beykock, in: The proteins, II, ed. J. Neurath (Academic Press, New York, NY, 1964) chap. 8.